JOURNAL OF SOLID STATE CHEMISTRY 59, 348–356 (1985)

Compounds of Molybdenum and Tungsten with High Specific Surface Area

II. Carbides

LEO VOLPE AND M. BOUDART[1]

Department of Chemical Engineering, Stanford University,
Stanford, California 94305

Received December 14, 1984

Temperature-programmed carburization of W_2N and Mo_2N powders in CH_4–H_2 mixtures up to 1150 and 970 K, respectively, leads to metastable face-centered cubic carbide phases. The reaction is topotactic in the sense that the face-centered cubic structure of the metal atoms remains unaltered, while the nitrogen and carbon atoms exchange their interstitial positions. Thus, the product retains the structure, crystallite size, and high specific surface area of its nitride parent, namely, 55 and 185 $m^2\ g^{-1}$ for β-WC_{1-x} and α-$MoC_{0.45}$, respectively.

Introduction

Among interstitial alloys of transition metals, carbides of tungsten and molybdenum are known for their extreme hardness, thermal stability, and surface reactivity in heterogeneous catalysis (*1*, *2*). This paper describes an easy means to prepare uncommon metastable phases of these materials in the form of unsupported powders with very high specific surface area (S_g).

The properties of the carbides depend on their electronic structure and bonding. Much of the attention in the literature has been paid to experimental determination of the direction of charge transfer between the metal and carbon and theoretical description of bonding in terms of the band structure. Ramqvist *et al.* (*3–6*), using a combination of X-ray techniques, obtained reliable results on transition-metal carbides, nitrides, and oxides. Their measurements indicated that the nonmetal atom carried a negative charge, in accord with Pauling's electronegativity scale. This view is supported by many recent self-consistent band calculations, such as those of Colot (*7*).

Band calculations by Dempsey (*8*) and Costa and Conte (*9*) correlated electrical and magnetic properties of transition-metal compounds, as well as the properties associated with cohesive energy, with filling of the metal *d*-band, first its bonding and then its antibonding portion. The results of those calculations implied, on the contrary, that the filling occurred by electron donation from nonmetal to metal.

Recently, Siegel (*10*) and Williams *et al.* (*11*) resolved the contradiction of charge transfer by demonstrating that electron donation to the nonmetal and filling of the *d*-band were not mutually exclusive. They used the notion of Heine (*12*) that the width of the *d*-band is inversely proportional to the fifth power of the metal–metal distance.

---

[1] To whom queries should be addressed.

0022-4596/85 $3.00

The lattice parameter is generally higher for the alloy than for the parent metal, and, therefore, the compound has a narrower band. Such a band can lose electrons to the nonmetal and yet be filled to a higher extent than the broader band of the parent. Thus, in the carbides, although there is little charge transfer relative to the free atoms, the *d*-band is enriched in electrons upon forming a compound.

The bonding properties of the surface and the bulk are generally different but related. Surface chemistry of the stable carbide phases, α-WC, W_2C, and Mo_2C, has received attention in catalysis and electrocatalysis, and connections between the reactivity and electronic structure have been reviewed (*2, 13*). Levy and Boudart (*14*) suggested Pt-like behavior of WC in H_2 oxidation and neopentane isomerization as if interstitial carbon had contributed to the filling of the *d*-band of W. The fact that in making and breaking C–C bonds Mo_2C behaves much like Ru (*15, 16*) supports this notion. In the light of modern band theory, the modified *d*-band seems to be filled to a higher extent than the band of the parent metal as a result of the presence of interstitial carbon, which thus confers to the group VI metals some of the chemical reactivity of group VIII metals.

Although several carbide phases other than α-WC, W_2C, and Mo_2C are known, their properties remain largely unexplored because they are difficult to synthesize. The materials of interest here are the face-centered cubic (fcc) carbides β-WC_{1-x} (*17*) and α-MoC_{1-x} (*18*), discovered in the early 1960s. These phases exhibit some deviation from stoichiometry (x is always positive). The fcc phases are also very refractory. Their melting points and microhardness values—2400 kg mm^{-2} for β-WC_{1-x} (*19*) and 1900–2600 kg mm^{-2} for α-MoC_{1-x} (*20*)—are at least as high as those of α-WC and Mo_2C. Unlike the common phases, the fcc compounds are superconductors, with superconducting transition temperatures of 10 and 14.3 K (*21*).

These carbides can be obtained at low temperatures only by rapid quenching of W–C and Mo–C mixtures from temperatures above 2798 and 2233 K, respectively, where they are thermodynamically stable. Other high-temperature preparation methods include diffusion welding in a glow discharge and hot pressing of a WC–Co alloy with W (*19*), reaction between MoO_3 and graphite in Ar-plasma arc or jet (*22*), and shock-wave detonations of Mo–C mixtures (*20*). The only reported method of preparation at low temperature involves $W(CO)_6$ or $Mo(CO)_6$ decomposition in H_2 around 700 K (*23*). All of these preparation methods typically lead to mixtures of β-WC_{1-x} or α-MoC_{1-x} with other phases.

To be used efficiently, a catalytic solid must be generally prepared with a high S_g, and inability to achieve it has been a major factor limiting the application of interstitial alloys of tungsten and molybdenum in catalysis (*2*). In a companion paper (*24*), we report that temperature-programmed reactions of WO_3 and MoO_3 with NH_3 can produce unsupported stable powders β-W_2N and γ-Mo_2N with S_g as high as 91 and 220 $m^2\,g^{-1}$, respectively, corresponding to a particle size of 3–4 nm. This study relates how the nitride powders can be transformed into the corresponding fcc carbides of high S_g upon low-temperature reaction with methane.

Experimental

The powders were prepared at atmospheric pressure by downflow of reactive gases through packed beds of W_2N or Mo_2N. The gases were CH_4 [Matheson, 99.97%, deoxygenated by passage through an MnO trap (*25*)] or H_2 (Pd-diffused) or both. The nitride parents had been synthesized by reacting WO_3 (99.999%) or MoO_3 (99.998%) powders with NH_3. The details of these processes and the characterization of the products are described elsewhere (*24*). The experiments employed about 0.5 g of solid precursor. The nitrides were carburized in the same quartz reactor in which they had been produced, without intermediate exposure to air. The temperature in the bed could be varied in a furnace and monitored locally with a thermocouple.

Presence of gas products at the reactor exit was determined qualitatively with a gas chromatograph (Aerograph 1520), equipped with a TC detector. Methane was separated from N_2 (He carrier gas) or H_2 (Ar carrier gas) in a Porapak "Q" column at room temperature (RT). Alternatively, the gas stream was analyzed for NH_3 with the help of an NDIR spectrophotometer (Beckman 865). The rate of CH_4 flow was measured with a rotameter, and the total flow rate was determined at the reactor exit with a soap-film flow meter. The latter flow rate was on the order of 10^2 μmol s^{-1} and held constant in all experiments.

The flow reactor was a part of a cell designed to measure *in situ* adsorption on the solid. Gas adsorption experiments were performed in a highly precise volumetric adsorption system (*26*). Following sample evacuation at 700 K to 10^{-4} Pa, a CO (Matheson, 99.995%) or H_2 adsorption isotherm was obtained at RT. Then the sample was evacuated to 10^{-4} Pa again to remove the gas weakly adsorbed at RT. Finally, the second CO adsorption isotherm was taken at RT. Afterward, N_2 (Matheson, 99.998%) adsorption was measured at liquid-N_2 temperature to determine the S_g using the standard BET method (*27*). Before exposure to air, all samples were passivated with a flowing mixture of 1% O_2 in He.

The bulk structure of the materials was determined by the standard powder X-ray diffractometric technique. This included crystallite-size estimation from X-ray diffraction (XRD) line broadening (*24*).

The elemental composition of the samples was measured at the Stanford Microanalytical Laboratory.

Results

Syntheses of the carbides β-WC_{1-x} and α-MoC_{1-x} were accomplished by temperature-programmed reactions (Fig. 1). The reactants were high-S_g W_2N and Mo_2N, as well as a sample of Mo_2N with small S_g, designated as Mo_2N-S (Table I). Methane treatment of the tungsten nitride below 850 K or of molybdenum nitride below 670 K did not lead to any observable reaction. Above these temperatures, H_2, N_2, and NH_3 were detected at the reactor exit. As the temperature slowly increased, so did the amounts of these three gases. Their concentrations went through very broad maxima around 1070 and 800 K for the tungsten and molybdenum compounds, respectively. At the final temperatures of 1150 and 970 K, no N_2 or NH_3 could be detected anymore, and the H_2 content had sharply fallen. None of the gas-phase concentrations was determined quantitatively.

Aqua regia and hot concentrated HNO_3 solution are known to dissolve the carbides completely (*29*). The products of our reac-

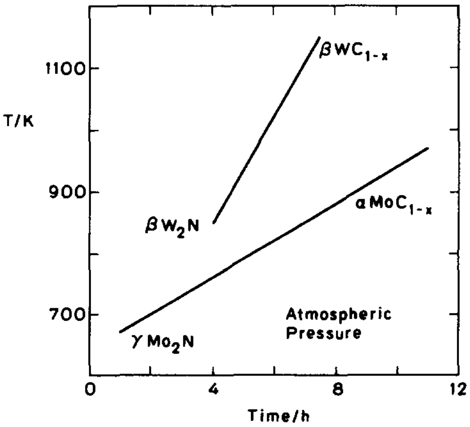

FIG. 1. Temperature-programmed synthesis of fcc carbides from the nitride powders of tungsten and molybdenum in the presence of CH_4.

TABLE I

PROPERTIES OF TUNGSTEN AND MOLYBDENUM NITRIDES BEFORE CARBURIZATION

Sample	a_{cub}[a] (pm)	S_g (m^2 g^{-1})	CO uptake (μmol g^{-1})	d_c (nm)
β-W_2N	412 ± 1	76[b]	180	4
γ-Mo_2N	416 ± 1	190[b]	970	6
γ-Mo_2N-S	416	20	—	20

[a] Lattice parameter of the fcc phases determined by XRD.

[b] Measured following CO adsorption and evacuation at RT. Carbon monoxide irreversibly chemisorbed at RT decreases the S_g of the nitrides by more than 10% (*24*).

tions, however, left free carbon as a residue in both solutions. Therefore, bulk free carbon was another product of the reactions.

Both transformations to carbide were accompanied by large decreases in S_g. This is shown in Table II, together with other properties of the fresh products.

Then we passed H_2 at 1000 and 870 K through the beds of our β-WC_{1-x} and α-MoC_{1-x} samples, respectively. Methane appeared at the reactor exit; its concentration increased and reached a maximum value in approximately 2 h, at which point the reactor was quenched to RT. The H_2 treatment did not alter the structure and crystallite size of the fcc phases, and no new phases appeared in the XRD patterns. The only effect was a 6 pm decrease in the lattice parameter of β-WC_{1-x} to 418 ± 1 pm. The tungsten carbide sample contained free carbon as it did before the H_2 treatment, but no free carbon could be detected in its molybdenum counterpart.

The reaction with H_2 restored much of the S_g lost during the nitride's carburization (Table II). The amount of CO chemisorption was found by extrapolating the isotherms to zero pressure. The fraction of CO that could not be evacuated at RT is chemisorbed irreversibly at that temperature. The data are presented in Table III. Note that the fresh carbide samples prior to H_2 treatment were not able to chemisorb CO.

After exposure to air, β-MoC_{1-x} contained 11.33, 0.27, and 0.4 wt% of C, N, and H; and the α-MoC_{1-x} sample had 5.03, 0.34, and 0.52 wt% of C, N, and H. The powders were not analyzed for metal and oxygen contents.

In a separate experiment, an identical Mo_2N sample was carburized following the temperature–time program in Fig. 1 with a 1 : 4 CH_4–H_2 mixture, rather than with CH_4 alone. The XRD pattern, S_g, and CO uptake of the final product were similar to those of the α-MoC_{1-x} sample prepared by sequential carburization with CH_4 and isothermal H_2 treatment. No free carbon was found in the reactor after the synthesis.

Another carburization experiment was

TABLE II

CRYSTAL PROPERTIES AND S_g VALUES OF THE FCC CARBIDES PREPARED BY CARBURIZATION OF W AND Mo NITRIDES

			S_g (m^2 g^{-1})	
Sample	a_{cub} (pm)	d_c (nm)	After CH_4 treatment	CH_4 and H_2 treatments
β-WC_{1-x}	418 ± 1[a]	4	30	55
α-MoC	423 ± 1	6	150	185
α-MoC_{1-x}-S	423	20	—	20

[a] Following H_2 treatment. After initial carburization with CH_4, the parameter was 6 pm higher.

TABLE III

SELECTIVE CHEMISORPTION ON THE CARBIDE POWDERS OF W AND Mo[a]

	Chemisorption (μmol g^{-1})			
Sample	CO	H_2	n_{CO} (10^{14} cm^{-2})	n_{H_2} (10^{14} cm^{-2})
β-WC	137	98	1.51	1.08
α-MoC_{1-x}	950	—	3.09	—
α-MoC_{1-x}-S	178	—	5.26	—

[a] Amounts of total and irreversible chemisorption for tungsten and molybdenum carbides, respectively.

done with a sintered Mo_2N sample. The sintering involved heating the high-S_g Mo_2N powder at 1070 K in flowing N_2 (passed through the MnO trap and a 0.5-nm molecular sieve trap at dry-ice temperature) for 12 h. The sintered nitride, Mo_2N-S, had an S_g of 20 m^2 g^{-1} and crystallite size of ca. 20 nm. This sample, too, was reacted with a 1:4 CH_4–H_2 mixture in the same way as the high-S_g powder. The treatment produced a carbide, α-MoC_{1-x}-S, having an fcc lattice with the same parameter, a_{cub} = 423 pm, as the high-S_g product. The values of S_g and crystallite size were equal to those of its parent Mo_2N-S (Table II). The amount of CO chemisorption is given in Table III. Again, free carbon was absent after the synthesis. Indeed, the product dissolved in *aqua regia* without a residue.

Discussion

The phase diagrams of the W–C and Mo–C systems (*17, 30*) are shown in Fig. 2. Below 2798 K the stable tungsten carbide phases include α-WC (WC structure, simple hexagonal) and W_2C (hexagonal closest-packed arrangement of the metal atoms or hcp). In the Mo–C system, only Mo_2C (isostructural with W_2C) is stable thermodynamically below 1928 K. It was determined by neutron diffraction (*31*) that the low-temperature α-M_2C structures (M = W or Mo) have an ordered arrangement of the C atoms, which makes them only pseudo-hcp.

At higher temperatures, other carbides are found on the phase diagrams. They all, except α-WC, have wide composition ranges and involve closest packing of the metal atoms where carbon atoms are randomly distributed among the octahedral interstices. Their structures are given in Table IV. The structural differences lie only in the stacking sequence of closest-packed layers as illustrated in Fig. 3: A, A for WC;

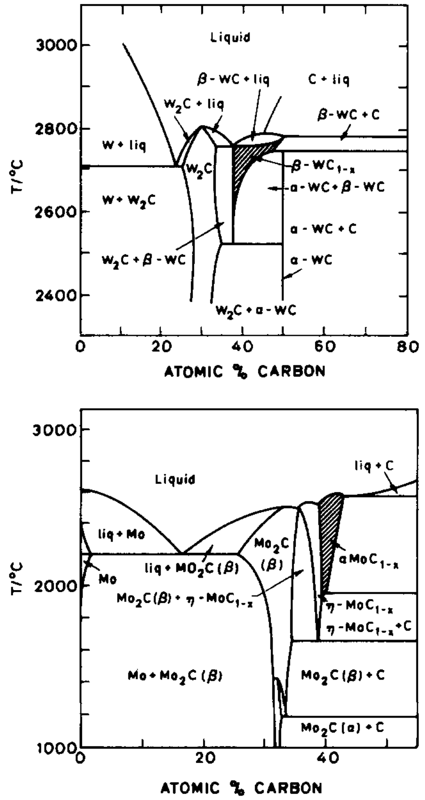

FIG. 2. Phase diagrams of the W–C (*17*) and Mo–C (*30*) systems, adapted with permission from the authors. The fcc carbides are cross-hatched.

TABLE IV

CRYSTAL STRUCTURES AND LATTICE PARAMETERS OF THE HIGH-TEMPERATURE PHASES IN THE W–C AND MO–C SYSTEMS

Phase	Structure	Lattice parameters (pm)	a_{nn}[a] (pm)
W_2C	hcp	a_{hex} = 300 (*1*) c_{hex} = 473	300
β-WC_{1-x}	fcc	a_{cub} = 422 (*1*) 412.5 (*17*)	298 292
α-WC	WC-type	a_{hex} = 291 (*1*) c_{hex} = 284	291 284
Mo_2C	hcp	a_{hex} = 300–301 (*30*) c_{hex} = 473–478	300
η-MoC_{1-x}	η-MoC-type	a_{hex} = 301 (*30*) c_{hex} = 1464	301
α-MoC_{1-x}	fcc	a_{cub} = 427 (*18*) 415 (*23*)	301 293

[a] In the last column, a_{nn} stands for the nearest-neighbor distance between the metal atoms.

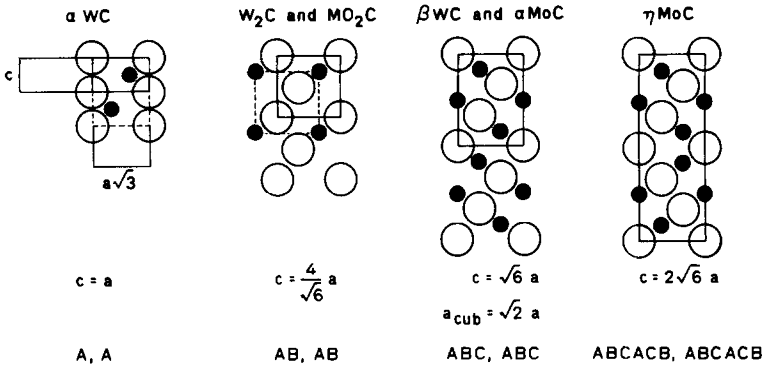

FIG. 3. Structure of tungsten and molybdenum carbides. The metal and carbon atoms are represented by open and dark circles, respectively. The stacking sequence of closest-packed layers is shown vertically, so that the unit-cell dimension within each layer, *a*, equals the nearest-neighbor distance. All the phases are idealized as stoichiometric.

AB, AB, for hcp structures; ABC, ABC for fcc ones; and ABCACB, ABCACB for η-MoC_{1-x}. Although the interatomic distances and, consequently, the sizes of the interstitial sites of the phases differ little, the fcc phases tend to be richer in carbon than the hcp ones. The lattice dimensions of β-WC_{1-x} and α-MoC_{1-x} expand with increases in the carbon/metal ratio.

Thermodynamically stable carbides invariably result from carburization of W, Mo, or their compounds. Common carbon sources include graphite, hydrocarbons, and CO. At the conditions of our carburization experiments α-M_2C and α-WC are expected to form. Our results, however, belie the expectation—both products turn out to be metastable fcc carbides. They seem identical to the high-temperature phases. As far as a_{cub} is concerned, our carbide samples are indistinguishable from those synthesized by other methods (Tables II and IV). The stoichiometry in our samples is unclear. Since carbides are not known to dissolve H (*1*), and hydrocarbons crack at high temperature, we can suppose that all the hydrogen contained in the samples is in the form of adsorbed water. With this assumption, the approximate composition of our tungsten carbide powder corresponds to $WC_{2.0}$. Hence, at least half of the carbon must be free. The molybdenum carbide formula is $MoC_{0.45}$, and all its carbon appears to be carbidic.

Graphite formation by CH_4 decomposition is favored thermodynamically for CH_4–H_2 mixtures with more than 12% of methane at 970 K and more than 3% at 1150 K, our highest process temperatures. When the nitrides are treated with CH_4 alone, bulk free carbon is indeed produced. Yet it is absent with 20% CH_4 in H_2 in the case of Mo_2N carburization. Clearly, kinetic factors are dominating.

In a kinetic sense, the carburization of W_2N and Mo_2N involves many elementary processes. The following steps inevitably take part in the reaction: adsorption and subsequent catalytic decomposition of CH_4, diffusion of N out of the solid, diffusion of C into the solid, associative desorption of N_2, and/or hydrogenation of N to NH_3. Besides, in CH_4-rich mixtures bulk free carbon is formed (creation of C–C bonds), and in CH_4-lean mixtures H_2 adsorbs on the surface and suppresses free-carbon buildup. In the absence of methane, H_2 removes surface carbon.

Despite, and apart from, the numerous interfacial processes, the solid-state transformation appears to be remarkably simple. It requires movement of nonmetal atoms only. Thus, the N atoms diffuse out, and the C atoms move in to take their place, while the metal atoms remain essentially motionless as their fcc structure stays unaltered. Only the distance between the nearest W and Mo neighbors increases by 12 and 7 pm, respectively.

Low-temperature diffusion data for interstitial nonmetal atoms in the carbides and nitrides are unavailable. These results indicate that such atoms can diffuse at appreciable rates at our process conditions. Thus, carbon atoms can diffuse toward the surface of a large WC single crystal at 1100 K upon removal of surface carbon (*32*).

Were the metal atoms allowed to move, nothing would prevent them from "restacking" the closest-packed layers to yield the stable hexagonal phases. Apparently, the process temperatures are insufficiently high for the W or Mo atoms to diffuse. According to the Tammann criteria (*33*), bulk and surface diffusion should occur at temperatures higher than $\frac{1}{2}$ and $\frac{1}{3}$ of the melting point, respectively. The carbides of W and Mo melt above 3050 and 2800 K. The values for the nitrides are unknown but expected to be very high as well, and, therefore, the immobility of the metal atoms offers no surprise.

Our results show that no sintering takes place as a result of the diffusion of interstitial N and C atoms through the solid. Indeed, the nitride-to-carbide transformation does not change the crystallite size. The S_g values of the Mo_2N samples, both the original and the sintered ones, are retained in the case of CH_4–H_2 treatment. With CH_4 alone, the S_g of W_2N and Mo_2N decrease due to clogging of the pores, known to be narrow (*24*), rather than to sintering. This is why "recovery" of S_g takes place during the subsequent carbon hydrogenation.

The nitride-to-carbide transformation belongs to the class of topotactic reactions (*34*) because of the crystal-lattice relationship between the parent and the product throughout the bulk of the solid. Usually, topotaxy preserves only certain structural motives, but here the carbides take over the fcc lattice of the nitrides entirely. A topotactic process starts with oriented nucleation of the product phase relative to the parent crystal. Therefore, our case, which requires no rearrangement of the metal atoms, provides an ideal example of topotaxy. As a typical topotactic reaction, this process is characterized by restricted mobility of species in the solid and leads, ultimately, to metastable products unattainable by common preparation methods.

Upon diffusion to the surface, nitrogen can desorb as N_2 or react with hydrogen and leave as NH_3. The NH_3/N_2 ratio is unknown and is likely to depend on experimental conditions and to vary within the packed bed. Quantitative composition measurements of the gas phase are required to determine the details of nitrogen removal.

Surface Reactivity

Prior to this investigation, there had been little opportunity and hardly any incentive to study surface reactivity of the fcc carbides of tungsten and molybdenum, uncommon materials difficult to prepare and almost impossible to isolate from other phases. This work provides a novel, easily accessible route to β-WC_{1-x} and α-MoC_{1-x}, and their high S_g adds a motivation of applying them as heterogeneous catalysts.

Our results on gas chemisorption (Table III) provide a preliminary indication of the surface reactivity of the carbides. The number densities, n_{CO} and n_{H_2}, for molecules chemisorbed at RT are calculated as the uptake per unit BET S_g. We can expect the density of the metal atoms on a clean carbide surface, n_W or n_{Mo}, to be 1.1×10^{15} cm^{-2}, assuming that the surface consists of equal proportions of the low-index planes. On β-WC_{1-x}, n_{CO} and n_{H_2} correspond to 14 and 11% of n_W. On α-MoC_{1-x} and α-MoC_{1-x}-S, the values of n_{CO} are close to 30 and 50% of n_{Mo}, respectively.

The low n_{H_2} value is consistent with the results of Benziger *et al.* (*35*) on a partially carburized W(100) face. Surface carburization of W(100) and Mo(100) (*36*) completely suppresses CO dissociation but allows molecular adsorption of a full CO monolayer at 200 K. All of it can be removed by flash desportion below 400 K, suggesting that the RT uptake may be smaller than a monolayer. Therefore, the values of n_{CO} on the molybdenum-carbide samples are reasonable for a clean surface. The low CO uptake by β-WC_{1-x} could be caused by surface contamination with free carbon. In any case, our n_{CO} and n_{H_2} values are higher than any reported previously for reduced carbide powders of tungsten or molybdenum.

Conclusions

Reactions of β-W_2N and γ-Mo_2N with CH_4 provide a novel method to prepare the fcc carbide phases β-WC_{1-x} and α-MoC_{1-x}. The crystallite size of the parent nitride is retained in the process, and so is the S_g unless the solid's pores become clogged with carbon. This gives the opportunity to synthesize β-WC_{1-x} and α-$MoC_{0.45}$ of 55 and 185 $m^2\ g^{-1}$, respectively, from the already available high-S_g powders.

The most remarkable feature of the solid-state reaction is the immobility of the metal atoms. The carbides simply inherit the fcc arrangement of the W or Mo atoms of the nitrides, while the nitrogen atoms in the octahedral interstitial sites diffuse out and are replaced by carbon atoms that diffuse into the crystal. In the process, the lattice expands only by 1–3% adopting the parameters a_{cub} = 418–424 pm in β-WC_{1-x} (x remains to be determined) and 423 pm in α-$MoC_{0.45}$. The fcc carbides would be thermodynamically stable at temperatures much higher than those used in our process. The limited mobility of species in the solid, retention of structural features, and metastability of products are all the marks of a topotactic reaction.

Acknowledgments

We thank J. S. Lee and S. T. Oyama for assistance and advice. The investigation was initiated with support from the Center for Materials Research at Stanford University under the NSF-MRL Program (NSF-DMR 80-20248-A2).

References

1. L. E. Toth, "Transition Metal Carbides and Nitrides," Academic Press, New York (1971).
2. S. T. Oyama and G. L. Haller, *in* "Catalysis" (A Specialist Periodical Report, Royal Society of Chemistry), Vol. 5, p. 333, Alden Press, Oxford (1982).
3. L. Ramqvist, K. Hamrin, G. Johansson, H. Gelius, and C. Nordling, *J. Phys. Chem. Solids* **31,** 2669 (1970).
4. L. Ramqvist, K. Hamrin, G. Johansson, A. Fahlman, and C. Nordling, *J. Phys. Chem. Solids* **30,** 1835 (1969).
5. L. Ramqvist, *J. Phys. Chem. Solids* **48,** 119 (1971).
6. L. Ramqvist, *J. Appl. Phys.* **42,** 2113 (1971).
7. J. L. Colot, *J. Phys. C* **10,** 1675 (1977).
8. E. Dempsey, *Philos. Mag.* **8,** 285 (1963).
9. P. Costa and R. R. Conte, *in* "Compounds of Interest to Nuclear Reactor Technology," Inst. Metals, Spec. Rep. No. 13 (J. T. Waber, P. Chiotli, and W. N. Miner, Eds.), Edwards, Ann Arbor, Mich. (1967).
10. E. Siegel, *Semicond. Insul.* **5,** 47 (1979).
11. A. R. Williams, C. D. Gelatt, J. W. D. Connolly, and V. L. Moruzzi, *Mater. Res. Soc. Symp. Proc.* **19,** 17 (1983).
12. V. Heine, *Phys. Rev.* **153,** 673 (1967).
13. R. B. Levy, *in* "Advanced Materials in Catalysis" (J. J. Burton and R. L. Garten, Eds.), p. 101, Academic Press, New York (1977).
14. R. B. Levy and M. Boudart, *Science* (*Washington, D.C.*) **181,** 547 (1973).
15. M. Boudart, S. T. Oyama, and L. Leclercq, *in* "Proceedings, 7th International Congress on Catalysis" (T. Seiyama and K. Tanabe, Eds.), p. 578, Elsevier, Amsterdam (1981).
16. J. S. Lee and M. Boudart, submitted.
17. R. V. Sara, *J. Amer. Ceram. Soc.* **48,** 251 (1965).
18. E. V. Clougherty, K. H. Lathrop, and J. A. Kafalas, *Nature* (*London*) **191,** 1194 (1961).

19. G. V. Samsonov, I. M. Muha, B. I. Kalnenko, and L. N. Pereselentseva, *Fiz. Khim. Obrab. Mater.,* 123 (1975).

20. V. P. Aleksevskii, L. P. Isaeva, V. I. Kovtun, M. D. Smolin, I. I. Timofeeva, and V. V. Yarosh, *Vys. Davleniya Svoistva Mater. Mater. Resp. Nauchn. Semin. 3rd,* 136 (1978).

21. R. H. Willens, E. Buehler, and B. T. Matthias, *Phys. Rev.* **159,** 327 (1967).

22. O. Matsumoto and Y. Yaguchi, *Commun.-Symp. Int. Chim. Plasmas, 3rd,* paper S.4.2. (1977).

23. A. A. Babad-Zakhryapin, L. T. Lysenko, and L. M. Gert, *Fiz. Met. Metalloved.* **21,** 782 (1966).

24. L. Volpe and M. Boudart, *J. Solid State Chem.* **59,** 332 (1985).

25. C. R. McIlwrick and C. S. G. Phillips, *J. Phys. E.* **6,** 1208 (1973).

26. F. V. Hanson, Ph.D. dissertation. Stanford University (1975).

27. S. Brunauer, P. H. Emmett, and E. Teller, *J. Amer. Chem. Soc.* **60,** 309 (1938).

28. S. F. Bartram, *in* "Handbook of X-Rays" (E. F. Kaelbe, Ed.), Chap. 17, McGraw–Hill, New York (1967).

29. G. V. Samsonov and I. M. Vinitskii, "Handbook of Refractory Compounds," Plenum, New York (1980).

30. E. Rudy, St. Windisch, A. J. Stosick, and J. R. Hoffman, *Trans. AIME* **239,** 1247 (1967).

31. E. Parthe and V. Sadagopan, *Acta Crystallogr.* **16,** 202 (1963).

32. P. M. Stefan, Ph.D. dissertation. Stanford University (1984).

33. G. Tammann, *Z. Anorg. Chem.* **149,** 67 (1925).

34. L. Volpe and M. Boudart, *Catal. Rev.-Sci. Eng.* **27,** 515 (1985).

35. J. B. Benziger, E. I. Ko, and R. J. Madix, *J. Catal.* **54,** 414 (1978).

36. E. I. Ko and R. J. Madix, *Surf. Sci.* **109,** 221 (1981).